

USING CONTEXTUAL INFORMATION TO CLASSIFY NUCLEI IN HISTOLOGY IMAGES

Kien Nguyen, Joerg Bredno, David A. Knowles

Ventana Medical Systems, Inc., A member of Roche Group
Digital Pathology and Workflow
Mountain View, USA

ABSTRACT

Nucleus classification is a central task in digital pathology. Given a tissue image, our goal is to classify detected nuclei into different types, for example nuclei of tumor cells, stroma cells, or immune cells. State-of-the-art methods achieve this by extracting different types of features such as morphology, image intensities, and texture features in the nucleus regions. Such features are input to training and classification, e.g. using a support vector machine. In this paper, we introduce additional contextual information obtained from neighboring nuclei or texture in the surrounding tissue regions to improve nucleus classification. Three different methods are presented. These methods use conditional random fields (CRF), texture features computed in image patches centered at each nucleus, and a novel method based on the bag-of-words (BoW) model. The methods are evaluated on images of tumor-burdened tissue from H&E-stained and Ki-67-stained breast samples. The experimental results show that contextual information systematically improves classification accuracy. The proposed BoW-based method performs better than the CRF-based method, and requires less computation than the texture-feature-based method.

Index Terms— Nucleus classification, conditional random field, bag-of-words, digital pathology, Ki-67, H&E, IHC

1. INTRODUCTION

Quantitative tissue analysis frequently needs to detect and label cell nuclei according to type (tumor, immune, stroma, etc.) or response to immunohistochemistry (IHC) staining. Due to the very large number of nuclei present in a whole slide tissue image, it is infeasible for pathologists to manually perform the task. Hence, it is desirable to develop an automated system to detect and classify nuclei in these images.

Multiple approaches to nucleus classification have been presented. In the most recent study [1], a novel technique called gray level size zone matrix is proposed to compute texture information in the nuclei regions, and is applied to classify two different cell databases. In [2], the authors use shape descriptors and a manifold learning technique to distinguish true cell nuclei from spurious objects in H&E-stained

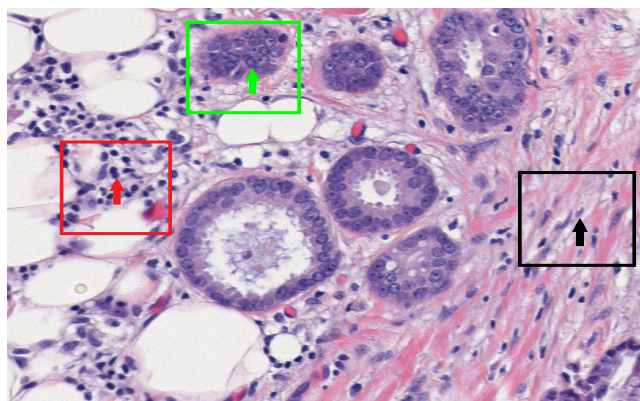


Fig. 1. Three classes of nuclei in H&E stained breast tissue specimens: tumor nuclei, lymphocytes, and stroma nuclei, indicated by green, red and black arrows, respectively. The rectangles denote the neighborhood regions of the nuclei indicated by the arrows.

prostate specimens. More often, both shape descriptors and texture features from nuclei regions are combined. This is used to identify cell cycle phases [3] and to classify cervical cells as normal or abnormal [4]. The basic method is extended in [5] to classify nuclei in diffuse gliomas. Here, intensity and gradient features in a small ribbon area surrounding the nuclei are computed in addition to shape and texture features, therefore extending the feature set with background features.

While the aforementioned studies focus on computing and evaluating isolated nuclear features from the nuclei regions, contextual information (CI) of the nuclei and cells are rarely considered or discussed in the nuclei classification literature¹. Intuitively, the CI of a nucleus of interest (NoI), i.e., information describing neighboring nuclei or the image texture in a region centered at the NoI provides useful evidence to predict its label. For example, a nucleus can be more confidently labeled as tumor provided that the neighboring nuclei are also tumor nuclei or the textural pattern of the surrounding area is similar to that in a tumor region. In Fig. 1, the green, black, and red rectangles indicate the neighborhood

¹ Although the studies [6, 7] use CI for nuclei classification (more specifically, they use the context-texture method that we will present in Sec. 3.1), they do not have any discussion or evaluation on CI as we do here.

areas that provide useful CI to classify the nuclei indicated by green, black and red arrows, respectively. In this paper, we explore three different methods to utilize this information: (i) the context-CRF method that employs the conditional random field (CRF) model to enhance the homogeneity of the classification result, (ii) the context-texture method that computes a rich set of texture features from the image patch centered at the NoI, and (iii) a novel context-BoW method that utilizes the bag-of-words (BoW) model to capture the appearance of neighboring nuclei.

Contributions of the paper:

1. We combine CI with a set of traditional *nuclear features* to improve classification accuracy over that achieved with nuclear features alone.
2. We propose a novel context-BoW method to extract CI and show that it (i) performs better than the context-CRF method, and (ii) requires lower computation cost than the context-texture method.
3. We perform comprehensive experiments on two different nucleus databases obtained from different staining methods.

2. NUCLEAR FEATURES

Nucleus centers are detected based on radial-symmetry voting [8]. Nuclei are segmented by thresholds individually computed for each nucleus using Otsu's method in a region around the nucleus. Nuclear features are computed for each nucleus and include:

1. *Morphology features*: area, minor and major axis lengths, perimeter, radius, and solidity.
2. *Appearance features*: the 10th, 50th and 95th percentile values (a method to estimate the min, mean and max values that is robust against noise) of pixel intensities and of gradient magnitudes computed from different image channels [9], namely Hematoxylin, luminance and either Eosin (for H&E-stained images) or DAB (for Ki-67 stained images) in the segmented nuclei area.
3. *Background features*: similar to the nuclear appearance features, but computed in a ribbon of 20 pixels ($\sim 9\mu m$) thickness around each nucleus boundary (which captures a sufficient amount of background tissue). These features are similar to those introduced in [5], where they are used to determine if the surrounding tissue is stroma or epithelium.

3. CONTEXT-AWARE METHODS

3.1. Context-Texture Method

The goal of this method is to capture the textural pattern in a region around each NoI. This may help to identify the local type of tissue in which the NoI is lying. Specific regions include solid tumor, aggregates of lymphocytes (immune cells), stroma, and overall staining responses. For example, stroma is characterized by a fiber-like texture, while the presence of

multiple blobs of varying size is characteristic for tumor regions. This is captured by contextual texture features computed in an image patch of size $S \times S$ centered at each nucleus. In this paper, we use $S = 150$ pixels ($\sim 70\mu m$), which captures a reasonably large tissue area that provides rich CI about the nuclei. This comparably large image patch to extract texture features distinguishes this method from most previously presented methods. The textual features are computed from the three different image channels described in Sec. 2, and include many popular texture features, namely histogram of intensities, histogram of gradient magnitude and gradient orientation, Gabor features, and Haralick features [10].

3.2. Context-CRF Method

In this method, the CRF model is used to promote homogeneity of labeling results, i.e., it encourages closely located nuclei to have the same labels. The motivation is that a homogeneous tissue region (tissue, stroma, etc.) usually contains nuclei of the same type. With $\mathbf{y} = \{y_1, y_2, \dots, y_N\}$ and $\mathbf{x} = \{x_1, x_2, \dots, x_N\}$ denoted as sets of all nucleus labels and nuclear feature vectors, respectively, the labeling problem is formalized as the optimization problem $\mathbf{y}^* = \arg \min_{\mathbf{y}} p(\mathbf{y}|\mathbf{x})$. Such problems are usually solved using a graph representation to factorize the probability distribution for efficient inference. Here, the relationship between the nuclei is modeled using a graph $G = (V, E)$, where each vertex $v_i \in V$ corresponds to a nucleus n_i . An edge $e_{ij} \in E$ is created between v_i and v_j if the distance between two nuclei n_i, n_j is less than d (we choose $d = S/2 = 75$ pixels so that the neighborhood area of each nucleus is the same as in the context-texture method). The \mathbf{y}^* are obtained by minimizing the Gibbs energy function

$$E(\mathbf{y}) = \sum_i \psi_u(y_i|x_i) + \alpha \sum_{(i,j)} \psi_p(y_i, y_j). \quad (1)$$

The unary potential $\psi_u(y_i|x_i)$ is computed as the negative log probability output of an SVM classifier. Using G , $\psi_p(y_i, y_j)$ is set to $\mathbb{I}[y_i \neq y_j]$ if there is an edge between v_i and v_j , otherwise $\psi_p(y_i, y_j) = 0$. The energy function is minimized using the graph cut approach [11]. In this method, the important parameter is the regularization parameter α (a larger value of α leads to a higher homogeneity of the labeling).

3.3. Context-BoW Method

This method uses the observation that the CI of a NoI can be described via the appearance of its neighbors. Again, neighbors are nuclei within a distance $d = 75$ pixels. To capture the appearance of neighbors as CI, the popular BoW model is used to quantize their appearance as follows (see Fig. 2).

1. Extract nuclear features of all nuclei in training images.
2. Perform a clustering procedure using the K-means algorithm on all the training nuclear features to obtain C clusters².

²Experiments in Sec. 4 show that the best accuracies are obtained when $C = 10$ and $C = 50$

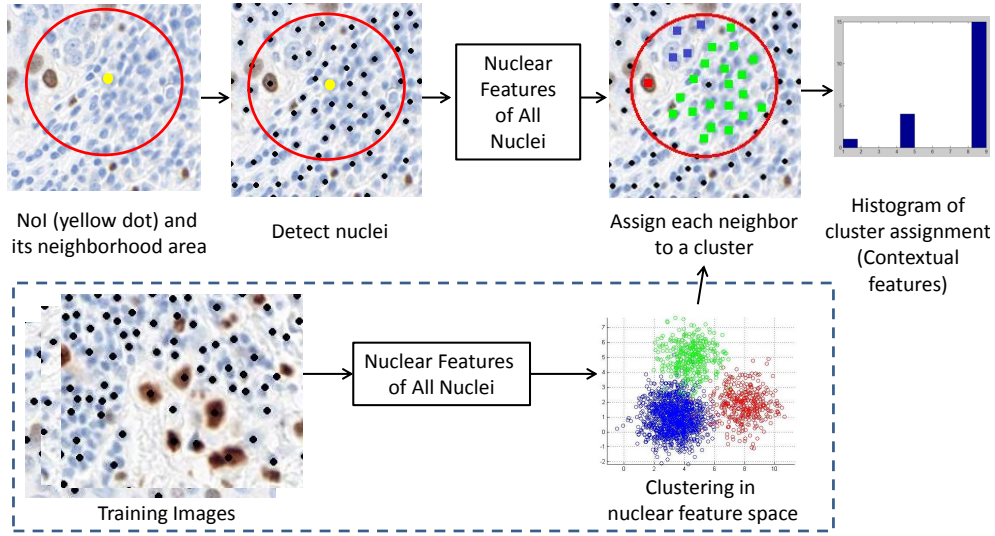


Fig. 2. Computing contextual features using the context-BoW method.

Database	Image description	Nuclei classes (number of nuclei)
H&E-stained images	75 images of $900 \times 1,000$ pixels, extracting from 25 tissue slides	Three classes: tumor (4,391), lymphocytes (509), and stroma (3,107)
Ki-67-stained images	96 images of $1,300 \times 1,000$ pixels, extracting from 29 tissue slides	Four classes: positive tumor (4,094), negative tumor (9,830), non-target stain (591), others (10,302)

Table 1. Description of the two different nucleus databases used for evaluation. The ground truth labels were determined by one pathologist for H&E database and one pathologist for Ki-67 database.

3. Given a NoI, assign its neighbors to the closest cluster centers using the Euclidean distance of each neighbor’s nuclear feature vector to the C centers, and compute a histogram of the cluster assignment. This histogram can be considered as contextual features of the NoI.

4. Combine the nuclear features and contextual features into a single feature vector for training and classification. As shown in Fig. 2, the cluster assignment of the nuclei in the neighborhood is a mean to describe the environment around the NoI.

4. EVALUATION

4.1. Database

A comprehensive evaluation of the three context-aware methods uses nucleus databases with the nuclei detected from tumor-burdened tissue from H&E-stained and Ki-67-stained breast samples. Slides were scanned on VENTANA iScan HT scanners, resulting in RGB wholeslide images with $0.465 \mu\text{m}$ pixel size. For H&E-stained tissue images, the goal is a clas-

Database	Nuclear features alone	Context-Texture	Context-CRF	Context-BoW
H&E	86.5 (13.3)	94.6 (4.1)	89.3 (10.1)	90.7 (7.0)
Ki-67	82.0 (8.1)	83.0 (9.0)	84.4 (7.3)	87.5 (9.2)

Table 2. Classification accuracies (s.d.) obtained by the three context-aware methods on the two different nuclei databases.

sification into nuclei of tumor cells, stroma cells, and lymphocytes (Fig. 1). For the Ki-67 stained tissue images (Fig. 3), the target classes are Ki-67-positive (proliferative) tumor nuclei, Ki-67-negative tumor nuclei, non-target staining responses (non-target stain), and the remaining Ki67-negative non-tumor nuclei (others). For this IHC staining, Ki-67-positive nuclei appear as brown blobs, while Ki-67-negative nuclei appear as blue blobs. The classification furthermore has to distinguish nuclei of tumor from non-tumor cells (in general tumor nuclei are larger than non-tumor nuclei). Table 1 summarizes the two databases.

A 10-fold image-based cross validation is performed for each database, and the average accuracies and standard deviations are reported. The nuclei in each image are used either for training or testing (nuclei are never tested with a model trained by nuclei taken from the same image). Similar to other studies in the literature, an SVM classifier is used.

4.2. Parameter Selection and Result

As mentioned above, the important parameter of the context-CRF method is the regularization parameter α , while that of the context-BoW method is the number of clusters C . For both databases, the the context-CRF method is tested with $\alpha \in [0.001, 0.01, 0.05, 0.1, 0.5, 1]$, while the context-BoW method is tested with $C \in [10, 30, 50, 70, 100, 150, 200]$ (Fig.

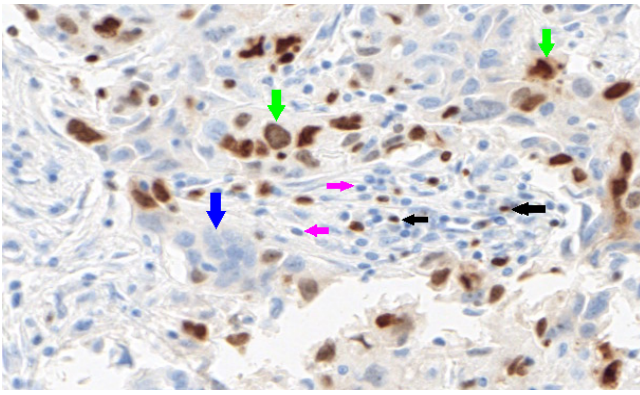


Fig. 3. Four classes of nuclei in Ki-67-stained breast tissue images: positive tumor, negative tumor, non-target stain, and others, indicated by green, blue, black, and pink arrows, respectively.

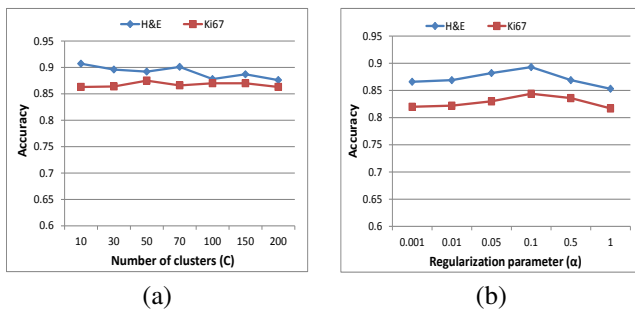


Fig. 4. Accuracies of the context-BoW and context-CRF methods depending on parameter choices. The parameters are (a) C for the context-BoW and (b) α for the context-CRF methods.

4). Final results (Table 2) are reported for parameter choices that result in best accuracies. For the context-texture method, the only important parameter is the patch size S . This parameter is fixed as 150 pixels so that it matches the parameter d in context-CRF and context-BoW methods. The same size of the local tissue neighborhood is enforced for fair comparisons. All classification accuracies are reported in Table 2. The results lead to the following main conclusions:

- Any use of CI leads to an improvement in nucleus classification accuracy.
- The proposed context-BoW method generally performs better than the context-CRF method (Table 2). These two methods are stable against parameter choices (Fig. 4).
- While the context-texture method obtains the best accuracy in the H&E nuclei databases, it requires the extra computation of texture features for the image patch centered at each nucleus, which is computationally expensive (a Matlab implementation of the features in Sec. 3.1 may take 1.1 seconds to process a nucleus). In contrast, the context-BoW and context-CRF methods utilize the pre-computed nuclear features and labels from the neighboring nuclei as CI, therefore allowing to incorporate CI with no additional feature extraction.

5. CONCLUSIONS

This paper presents different solutions for utilizing CI to classify nuclei in histology images. This useful information has not yet received sufficient attention in the literature. Three different methods are presented, including (i) the application of the popular CRF model on top of the nuclear features, (ii) the extraction of additional texture features in the image patches centered at the nuclei (and combining with the nuclear features), and (iii) a newly proposed method utilizing the BoW model to capture the appearance of the neighboring nuclei. This new method clusters the training nuclear features into a number of cluster centers, and assigns the neighbors of each NoI to these clusters. A histogram of cluster assignments of neighbors is combined with nuclear features to serve as the final feature vector for each NoI. A comprehensive evaluation shows that CI is useful for nucleus classification across two different image databases with very different stains. The newly proposed context-BoW method is attractive as it offers good classification accuracy at low computational cost, which is of relevance for the analysis of tissue samples that typically contain many tens of thousands of cell nuclei.

6. REFERENCES

- [1] G. Thibault, et al., "Advanced statistical matrices for texture characterization: Application to cell classification," *IEEE Trans. Biomed. Eng.*, vol. 61, pp. 630–637, 2014.
- [2] M. Arif and N. Rajpoot, "Classification of potential nuclei in prostate histology images using shape manifold learning," in *Int. Conf. on Machine Vision*, 2007, pp. 113–118.
- [3] M. Wang, et al., "Novel cell segmentation and online SVM for cell cycle phase identification in automated microscopy," *Bioinformatics*, vol. 24, pp. 94–101, 2008.
- [4] P. Marina and N. Christophoros, "Cervical cell classification based exclusively on nucleus features," in *Int. Conf. on Image Analysis and Recognition*, 2012, pp. 483–490.
- [5] J. Kong, et al., "A comprehensive framework for classification of nuclei in digital microscopy imaging: An application to diffuse gliomas," in *ISBI*, 2011, pp. 2128–2131.
- [6] S. Peter, et al., "Computational TMA analysis and cell nucleus classification of renal cell carcinoma," *Pattern Recognition*, vol. 6376, pp. 202–211, 2010.
- [7] K. Nguyen, A. Sarkar, and A. Jain, "Prostate cancer grading: Use of graph cut and spatial arrangement of nuclei," *IEEE Trans. Med. Imaging*, vol. PP, no. 99, pp. 1–1, 2014.
- [8] B. Parvin, et al., "Iterative voting for inference of structural saliency and characterization of subcellular events," *IEEE Transactions on Image Processing*, vol. 16, pp. 615–623, 2007.
- [9] A. Ruifrok and D. Johnston, "Quantification of histological staining by color deconvolution," *Anal. Quant. Cytol. Histol.*, vol. 23, pp. 291–299, 2001.
- [10] R. Haralick, K. Shanmugam, and I. Dinstein, "Textural features for image classification," *IEEE Trans. Syst. Man Cybern. SMC*, vol. 3, pp. 610–621, 1973.
- [11] Y. Boykov, et al., "Fast approximate energy minimization via graph cuts," *IEEE PAMI*, vol. 23, pp. 1222–1239, 2001.